

# The Biomechanics of Femoroacetabular Impingement

Daniel E. Martin, MD,\*† and Scott Tashman, PhD\*†‡

*From the \*University of Pittsburgh Medical Center Department of Orthopaedic Surgery, Pittsburgh, Pennsylvania; †University of Pittsburgh Biodynamics Laboratory, Pittsburgh, Pennsylvania; and ‡University of Pittsburgh School of Medicine, Pittsburgh, Pennsylvania.*

The authors have no conflicts to disclose. Reprint requests: Scott Tashman, PhD, University of Pittsburgh Biodynamics Laboratory, 3820 South Water Street, Pittsburgh, PA 15203, telephone: (412) 586-3950, fax: (412) 586-3979, email: tashman@pitt.edu

12 **Abstract:**

13 Femoroacetabular impingement (FAI) has been proposed as a possible biomechanical  
14 etiology of early, idiopathic hip osteoarthritis (OA). Two primary mechanisms have been  
15 proposed: cam impingement and pincer impingement. In cam impingement, an abnormally  
16 shaped or excessively large femoral head or neck abuts against the anterosuperior acetabulum. In  
17 pincer impingement, overcoverage of the proximal femur by the acetabulum results in  
18 impingement. In severe cases, a contre-coup mechanism has been suggested whereby an  
19 anterosuperior contact point functions as a fulcrum and posteroinferior impingement occurs as  
20 the femoral head is levered out of the acetabulum. However, these proposed mechanisms have  
21 been based on surgical observation rather than *in vivo* documentation of FAI, and controversy  
22 exists as to whether surgical interventions should be based on these theories alone. This review  
23 of FAI biomechanics discusses the proposed biomechanical mechanisms of FAI, the analytical  
24 methods currently available to study FAI biomechanics, and the topics that future biomechanical  
25 studies of FAI will need to address. Ultimately, better understanding the biomechanics of FAI  
26 may help physicians design interventions that decrease the risk of progression to hip OA.

27

28 **Key words:** Femoroacetabular impingement, hip biomechanics, cam impingement, pincer  
29 impingement.

30

31 **Introduction**

32 Femoroacetabular impingement (FAI) occurs when the head or neck of the femur abuts  
33 against the rim of the acetabulum. The principles of hip impingement have long been studied  
34 with regards to total hip arthroplasty (THA), in which components must be designed to minimize  
35 wear and dislocation [1-3]. Impingement has also been studied in congenital hip dysplasia and  
36 pediatric hip disorders, where dysmorphic native anatomy or surgically-altered anatomy provides  
37 a readily identifiable source of impingement [4-7]. The recognition of hip impingement in these  
38 patient populations has led several authors to examine FAI as a potential cause of early,  
39 idiopathic osteoarthritis (OA) in younger patients.

40 The work of Ganz et al. has been particularly instrumental in defining FAI, as this group  
41 has performed surgical dislocation of the hip in several hundred patients with symptomatic  
42 impingement and has meticulously documented their intraoperative observations [8-10]. These  
43 observations have provided the basis for two proposed mechanisms of femoroacetabular  
44 impingement: an abnormally shaped (non-spherical) or excessively large femoral head or neck,  
45 or overcoverage of the proximal femur by the acetabulum.

46 While these anatomic features can be easily recognized using readily available imaging  
47 techniques, such as plain radiographs, *in vivo* characterization of abnormal contact between the  
48 femur and the acetabulum has proven more difficult. Devising and implementing appropriate  
49 surgical interventions, therefore, has also been difficult. This review aims to summarize the  
50 proposed biomechanical mechanisms of FAI, the analytical methods currently available to study  
51 FAI biomechanics, and the topics that future biomechanical studies of FAI will need to address.

52

53 **Proposed Mechanisms of FAI**

54 Ganz et al. proposed FAI as a mechanism for the development of early OA in the absence  
55 of dysplasia after performing surgical dislocation of the hip on more than 600 symptomatic  
56 patients [9]. Based on the location of labral and articular cartilage pathology, the authors  
57 suggested that FAI occurred most often in terminal flexion, and that additional shearing damage  
58 could occur if terminal flexion was accompanied by rotation. Furthermore, the authors suggested  
59 that the impingement could result from two possible morphologic abnormalities, the cam lesion  
60 and the pincer lesion.

### 61 *Defining the Normal Hip*

62 In describing the biomechanical abnormalities, it is important to understand the criteria by  
63 which normal hip morphology is generally described, which has been drawn largely from the  
64 study of hip dysplasia [11]. The gold standard in clinical imaging of FAI is the magnetic  
65 resonance arthrogram, because it best identifies labral and cartilage pathology [12]. However,  
66 the following measures focus on the bony abnormalities presumed to cause FAI.

67 The center-edge angle (CEA) was developed to quantify hip dysplasia in which the  
68 acetabulum is too shallow, thus predisposing patients to instability of the hip joint. The CEA is  
69 measured on an anteroposterior (AP) radiograph of the hip as the angle between a vertical line  
70 that intersects the center of the femoral head and a line that is drawn from the center of the  
71 femoral head to the lateral-most aspect of the acetabulum (Figure 1A) [11]. A value greater than  
72 20 degrees is generally accepted to indicate a non-dysplastic hip. An AP radiograph of the hip  
73 can also be used to evaluate for the presence of a crossover sign, which denotes acetabular  
74 retroversion when the anterior rim of the acetabulum (which should be medial) runs more  
75 laterally in the most proximal part of the acetabulum and crosses the posterior rim distally [13].

76           The advent of magnetic resonance imaging (MRI) has allowed for more comprehensive  
77 evaluation of femoral head and neck morphology. The head of the femur is generally accepted to  
78 be shaped as a sphere that narrows to form the femoral neck. This narrowing provides an offset  
79 between the radius of the femoral head and that of the femoral neck, which allows for a greater  
80 range of motion about the hip (Figures 2A and 2B). The alpha angle has been proposed to  
81 evaluate deviations in the sphericity of the femoral head and the normal offset between the  
82 femoral head and the femoral neck [14]. The alpha angle is measured between a line parallel to  
83 the axis of the femoral neck and a line drawn from the center of the femoral head to the point at  
84 which the distance from the center of the femoral head to the cortex of the femoral head or neck  
85 first exceeds the radius of a circle fit to the femoral head (Figure 1B). While the values that  
86 indicate pathology are debated, values less than 50 degrees are generally accepted to represent  
87 normal proximal femur morphology.

88           Gosvig et al. have also recently proposed the triangular index (TI) for evaluation of  
89 proximal femoral morphology [15]. The TI is calculated by first fitting a circle to the femoral  
90 head and measuring the radius of the circle ( $r$ ). A line is next drawn along the longitudinal axis  
91 of the femoral neck, and then another line is drawn perpendicularly to this line at a distance of  $r/2$   
92 from the center of the femoral head. Finally, a triangle is drawn with a hypotenuse ( $R$ ) going  
93 from the center of the femoral head to the point at which the lateral cortex of the femur intersects  
94 the line previously drawn perpendicularly to the longitudinal axis of the femur (Figure 1C).  
95 When a radiograph with 1.2 times magnification is used, the proximal femur is classified as  
96 abnormal when  $R \geq r + 2$  mm. This method has the advantage of requiring only an AP  
97 radiograph, but its effectiveness has not been as thoroughly evaluated as the alpha angle.

98 *Cam Lesion*

99           A cam is a rotating or sliding piece in a mechanical linkage that translates rotary motion  
100 into linear motion or vice versa. This translation is generally caused by the rotation of an  
101 eccentrically shaped wheel, sphere, or cylinder. The femoral head is normally spherical and thus  
102 produces purely rotational movements. However, an abnormality in the shape of the femoral  
103 head or neck can disrupt these purely rotational movements to produce impingement or linear  
104 movement, hence the term “cam lesion” [2]. Some authors have also used the term “pistol grip  
105 deformity” when describing this lesion, due to the resulting appearance of the proximal femur on  
106 an anteroposterior (AP) radiograph [16].

107           The proposed mechanism of impingement in the presence of a cam lesion is impingement  
108 on the rim of the acetabulum by this abnormally shaped femoral head or neck in flexion (Figures  
109 2C and 2D) [9]. The impingement is proposed to produce symptoms by crushing the acetabular  
110 labrum that surrounds the acetabular rim, and by subsequently damaging the underlying articular  
111 cartilage [10].

#### 112 *Pincer Lesion*

113           Abnormality in the shape of the acetabulum, also known as a pincer lesion, is another  
114 suggested mechanism for FAI. A pincer is a hinged instrument with two short handles and two  
115 grasping jaws used for gripping. When there is overcoverage of the femoral head by the  
116 acetabulum, a cross-sectional image through the acetabulum makes the acetabulum appear like a  
117 pincer gripping the femoral head, rather than a cup in which the femoral head rests.  
118 Consequently, when a morphologically normal proximal femur is taken to the extremes of  
119 physiologically normal flexion in the presence of a pincer lesion, the rim of the acetabulum  
120 impinges on the neck of the femur (Figures 2E and 2F) [9].

121 Pincer impingement has been proposed to produce the same cascade of symptoms, with  
122 initial damage occurring at the acetabular labrum and subsequent damage occurring at the  
123 underlying articular cartilage. Although the etiology is unclear, pincer impingement has been  
124 observed to occur more often in women than in men [17].

#### 125 *Contre-Coup Mechanism*

126 The cam and pincer mechanisms have been proposed based on labral pathology in the  
127 location of anatomic abnormality, most commonly in the anterosuperior region of the  
128 acetabulum. However, some authors have reported surgical findings of additional labral  
129 pathology in the posteroinferior aspect of the acetabulum in the setting of more severe  
130 anterosuperior pathology [9, 10]. The authors propose that this occurs via a “contre-coup”  
131 mechanism, similar to a contre-coup head injury, in which a brain injury occurs opposite to the  
132 side of impact. In contre-coup impingement, the point of anterosuperior contact functions as a  
133 fulcrum by which the head of the femur is elevated out of the acetabulum and impacts at an  
134 opposite posteroinferior region of the acetabulum (Figures 2G and 2H). Because pincer  
135 impingement generally involves additional posterior overcoverage of the acetabulum, this  
136 posteroinferior pathology has been observed more often in patients with pincer impingement.  
137 However, this mechanism has only been proposed based on surgical findings, and no studies  
138 performed to date have been able to document its occurrence *in vivo*.

#### 139 *Findings on Physical Exam*

140 While a more thorough discussion of the clinical presentation of FAI is beyond the scope  
141 of this review, certain findings on physical exam correlate with the above detailed bony  
142 abnormalities. Klaue et al. first described the anterior impingement test in their description of  
143 the “acetabular rim syndrome” in 1991 [13]. This test consists of flexion, adduction, and internal

144 rotation of the hip, which places the anterior aspect of the femoral head/neck junction in contact  
145 with the anterosuperior acetabulum. The elicitation of pain is considered a positive test for  
146 impingement. Two tests can be used to test for posterior impingement. The posteroinferior  
147 impingement test is performed by placing a supine patient at the end of the examination table and  
148 allowing the affected hip to go into hyperextension. The affected leg is then externally rotated,  
149 with the elicitation of pain being considered a positive test for impingement [18]. The FABER  
150 (flexion, abduction, and external rotation) test is performed by placing the affected extremity of a  
151 supine patient in the figure-four position of flexion, abduction, and external rotation and then  
152 measuring the distance from the lateral aspect of the knee to the examination table [18]. An  
153 increased distance on the affected side from the lateral aspect of the knee to the examination  
154 table as compared to the unaffected side is considered a positive test for impingement.

155

## 156 **Research Techniques**

157 While the above findings have been documented, many unanswered questions remain.  
158 The underlying causes of the bony abnormalities have not been determined, and the mechanical  
159 mechanisms of impingement and resulting joint damage are not well understood. Research  
160 approaches for the study of FAI have consisted primarily of cadaveric biomechanical studies and  
161 static 2D or 3D imaging. A brief overview of some of these studies follows.

### 162 *Cadaveric Studies*

163 Given the recent development of surgical techniques for resection of the anterolateral  
164 aspect of the femoral neck to treat FAI presumed to be caused by a cam lesion [8, 19, 20],  
165 Mardones et al. evaluated the safety of such techniques with regard to the danger of femoral neck  
166 fracture. 15 matched pairs of cadaveric proximal femur specimens were divided into three



167 groups in which 10%, 30%, or 50% of the diameter of the femoral neck was excised. While the  
168 energy to fracture was inversely proportional to the amount of bone resection and the specimens  
169 in which 50% of the femoral neck was resected had a lower peak load to failure, no difference  
170 was observed between the 10% and 30% groups with regard to peak load to failure. The authors  
171 therefore suggested that no more than 30% of the femoral neck should be resected during  
172 osteoplasty. In a follow-up cadaveric study, they found that arthroscopic techniques resulted in  
173 resections of similar size to open techniques, but that arthroscopic techniques were less  
174 successful in performing the resection in the planned area [21]. Zumstein et al. documented  
175 similar difficulties in localizing the site of resection when arthroscopically resecting cadaveric  
176 acetabular rims [22].

#### 177 *Computed Tomography (CT)*

178 Beaulé et al. used three-dimensional CT to compare the proximal femoral morphology of  
179 30 subjects with painful non-dysplastic hips to that of 12 asymptomatic controls [23]. The mean  
180 alpha angle for the symptomatic group was found to be significantly greater in the symptomatic  
181 group than in the control group (66.4 vs 43.8,  $p = 0.001$ ). The mean alpha angle was also  
182 significantly greater for males in the symptomatic group than for females in the symptomatic  
183 group (73.3 versus 58.7,  $p = 0.009$ ). In addition to providing valuable demographic information,  
184 this study demonstrates that CT can be a useful and non-invasive method to study FAI.

185 Tannast et al. developed specialized software to predict hip range of motion in plastic  
186 models and cadaveric hips, based on CT bone models and validated using computer navigation  
187 software previously designed for hip arthroplasty [24]. The study demonstrated accuracy of  
188  $0.7 \pm 3.18$  degrees in a plastic bone setup and  $-5.0 \pm 5.68$  degrees in a cadaver setup, presumably  
189 due to soft tissue effects in the cadavers. The authors next used this software to predict the hip

190 range of motion of 21 subjects with FAI and 36 control subjects. Although a similar validation  
191 using the computer navigation software was not possible because the navigation software  
192 required the surgical implantation of reflective markers, the custom software predicted the  
193 expected deficits for symptomatic subjects in flexion and abduction from a neutral position and  
194 in internal rotation at 90 degrees of flexion (all  $p < 0.001$ ). Kubiak-Langer et al. applied the  
195 same research model to the prediction of the results of femoral neck osteoplasty in subjects with  
196 FAI and had similar success [25].

### 197 *Magnetic Resonance Imaging*

198 Wyss et al. studied the efficacy of MRI in predicting clinical symptoms by comparing the  
199 MRI findings and physical examinations of 23 subjects with FAI to those of 40 asymptomatic  
200 controls [26]. As expected, the authors found a significant decrease in hip internal rotation in the  
201 subjects with FAI compared to the controls ( $4 \pm 8$  degrees versus  $28 \pm 7$  degrees,  $p < 0.0001$ ).  
202 Interestingly, the authors found that there was a strong correlation between internal rotation and a  
203 measure that the authors devised to standardize the distance between the acetabular rim and  
204 potential zones of impingement on the femoral neck ( $r = 0.97$ ,  $p < 0.0001$ ). This measure, the  
205 beta angle, was defined as the angle between a line drawn on axial MRI from the center of the  
206 head of the femur to the lateral-most aspect of the acetabulum and a line drawn from the center  
207 of the head of the femur to the point where the distance from the bony cortex to the center of the  
208 femoral head first exceeded the radius of the femoral head (similar to the measurement used in  
209 the alpha angle).

### 210 *In Vivo Studies*

211 Kennedy et al. studied hip and pelvic motion in 17 subjects with FAI as compared to 14  
212 asymptomatic controls using reflective surface markers during level walking [27]. While the

213 authors were able to demonstrate decreased pelvic and hip motion in the sagittal and coronal  
214 planes in the FAI subjects as compared to the controls, this type of study does not allow for  
215 accurate assessment of joint contact during activities [28].

216

## 217 **Directions for Future Research**

218 The previously discussed studies have greatly expanded our understanding of the  
219 biomechanics of FAI, and hold great potential to translate this into improved clinical care. For  
220 example, cadaveric studies, such as those performed by Maradones et al. and Zumstein et al., are  
221 essential to ensure that novel surgical treatment of FAI can be performed safely [21, 22, 29].  
222 Furthermore, the prediction models of Kubiak-Langer et al. hold great potential for pre-operative  
223 planning and reproducible, quantitative assessment of surgical efficacy. However, future  
224 biomechanical studies should address two major shortcomings in our understanding of FAI: the  
225 etiology of the disorder and the nature of impinging joint motion that leads to tissue  
226 degeneration.

### 227 *The Etiology of FAI*

228 First, although femoroacetabular impingement has been characterized and several  
229 treatment options have already been developed, the underlying etiology of the observed bony  
230 abnormalities has not been determined. The potential etiologies of this “idiopathic” disease are  
231 widespread, ranging from early symptoms of osteoarthritis, to mild forms of pediatric disorders  
232 such as slipped capital femoral epiphysis that were unrecognized on initial presentation, to  
233 distinct diseases with as-yet unrecognized genetic or traumatic origins [30]. One potential tool to  
234 shed light on the underlying etiology of FAI is the application of more powerful computational  
235 models to the analysis of proximal femoral and acetabular morphology. While most previous

236 techniques have attempted to fit the shape of the head of the femur only to that of a circle on  
237 two-dimensional imaging, the work of Anderson et al. has expanded this principle to analyze  
238 deviations in the shape of the femoral head from a three-dimensional sphere using CT  
239 reconstructions [31]. This type of analysis holds great potential to help surgeons visualize  
240 complex three-dimensional deformities and allow them to use this information for pre-operative  
241 planning.

#### 242 *Characterizing the Mechanics of Impingement: In Vivo Imaging*

243 FAI is, by nature, a dynamic disorder whereby soft tissue damage results from abnormal  
244 motion of the femur relative to the acetabulum. Though extensive work has been conducted to  
245 characterize the bony abnormalities present in FAI and the ensuing clinical sequelae, no studies  
246 to date have imaged dynamic FAI *in vivo*. The hip joint is surrounded by large amounts of  
247 mobile soft tissue, and thus poorly suited to the most readily-available analytic technique, the  
248 attachment of reflective surface markers [28, 32, 33]. For similar reasons, the surgical  
249 attachment of reflective markers to bone would improve accuracy [34-38], but would be  
250 particularly morbid in this region. Surgical implantation of tantalum beads into bone to facilitate  
251 radiostereometric analysis (RSA) is another invasive technique that is generally reserved for  
252 patients already undergoing surgical intervention, and thus has not been applied to the native hip  
253 joint [39-41].

254 Dynamic biplane radiography in combination with model-based tracking is a recently  
255 developed technique that attempts to overcome these limitations. Briefly, this technique applies  
256 a ray-tracing algorithm to project simulated x-rays through a density-based, volumetric bone  
257 model (from a subject-specific CT scan), producing a digitally reconstructed radiograph (DRR).  
258 The *in-vivo* position and orientation of a bone is estimated by maximizing the correlation

259 between the DRRs and biplane x-ray images obtained during subject activity. By utilizing  
260 imaging equipment designed for high frame rates, dynamic joint function can be well  
261 characterized for a variety of joints and functional movement activities. This technique has  
262 previously been validated in the glenohumeral joint [42], the tibiofemoral joint [43], the  
263 patellofemoral joint [44], and, recently, in the hip joint [45].

264 Figure 3A presents an early subject with cam impingement in an ongoing study of FAI  
265 that employs model-based tracking and high-speed, biplane radiography. As seen in Figure 3B,  
266 labral pathology is already present although degenerative changes are not yet evident in Figure  
267 3A. Figure 4 demonstrates hip joint contact for the same subject at 40 and 60 degrees of hip  
268 flexion. As seen in Figure 4B, decreased anterosuperior joint space occurs at deeper flexion  
269 angles as a result of contact between the anterosuperior acetabulum and the anterior femoral  
270 head/neck junction. Although thresholds for predicting symptoms or for providing indications  
271 for operative intervention cannot be inferred from this early data, the results of this study will  
272 prove invaluable in determining the complex biomechanical interactions of the acetabulum and  
273 proximal femur during *in vivo* FAI.

274

## 275 **Conclusion**

276 FAI provides a difficult biomechanical puzzle to solve because the extensive soft tissue  
277 surrounding the hip joint has made accurate *in vivo* biomechanical studies difficult. Advances in  
278 imaging techniques have expanded our understanding of the cam, pincer, and contre-coup  
279 mechanisms of FAI, and new computational methods for analyzing acetabular and proximal  
280 femoral morphology may provide new clues to the underlying etiology of FAI. New *in vivo*  
281 analysis techniques such as model-based tracking and high-speed biplane radiograph will help

282 further characterize FAI and assist in the development of techniques for surgical intervention.  
283 Furthermore, these techniques will provide powerful tools with which to assess the efficacy of  
284 various interventions in restoring normal joint contact patterns.

285 **Acknowledgements**

286       The preliminary data presented in the paper was from an ongoing study funded by the 2008  
287 OREF/AAHKS/Zimmer Resident Clinician Scientist Training Grant in Total Joint Arthroplasty.

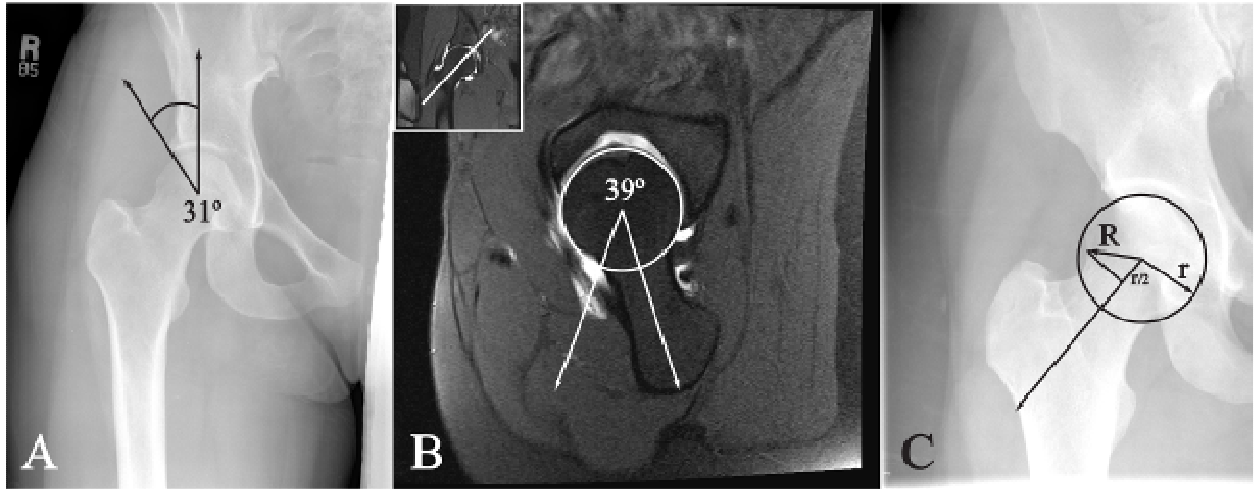
288

289 **Figures**

290



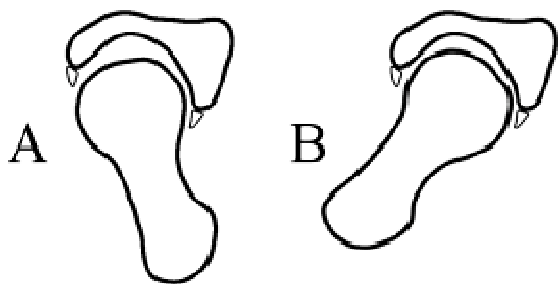
291 **Figure 1: Normal Hip Morphology**



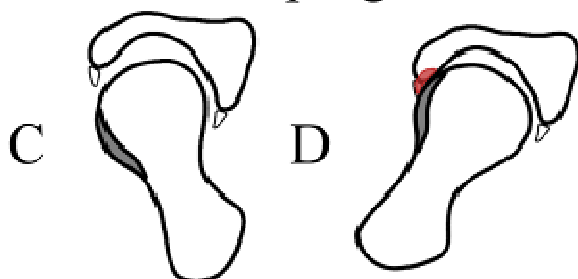
292

293

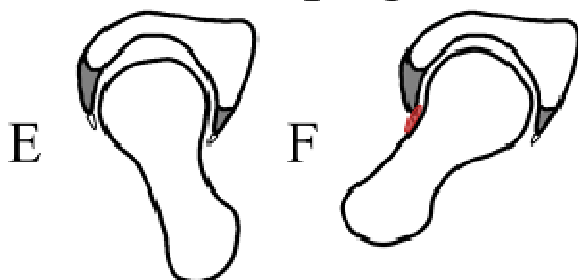
### Normal Joint



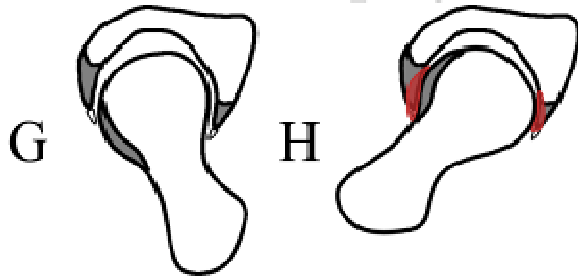
### Cam Impingement



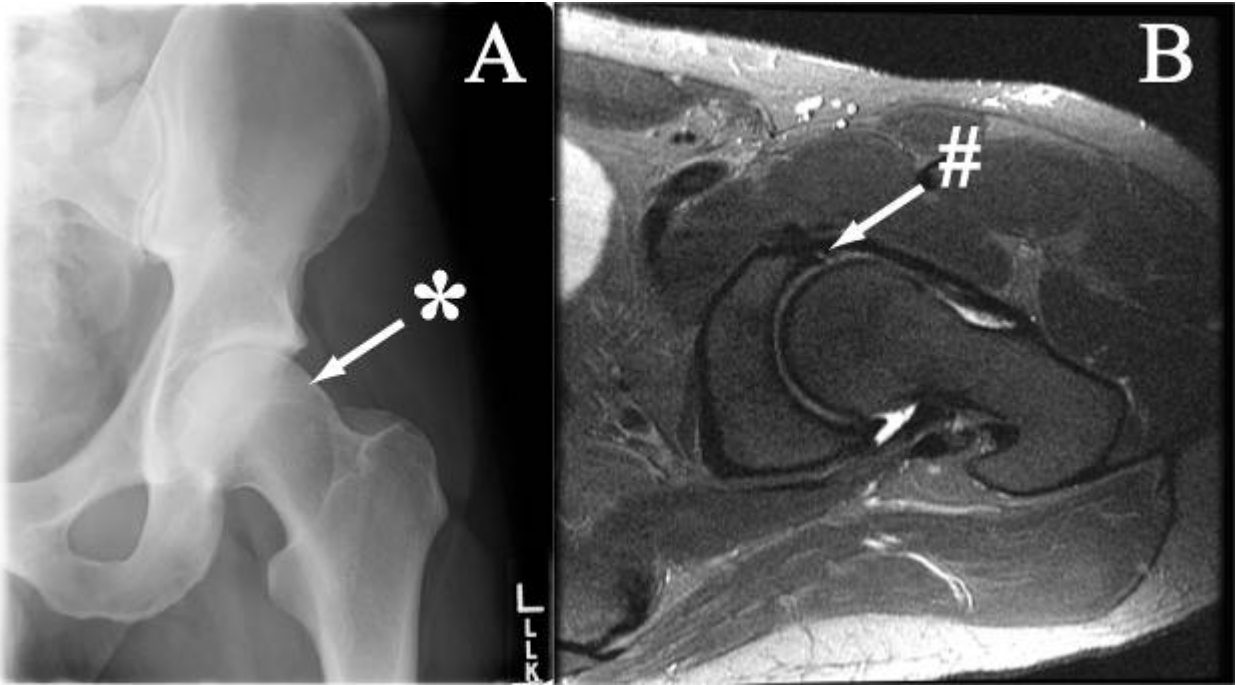
### Pincer Impingement



### Combined Impingement



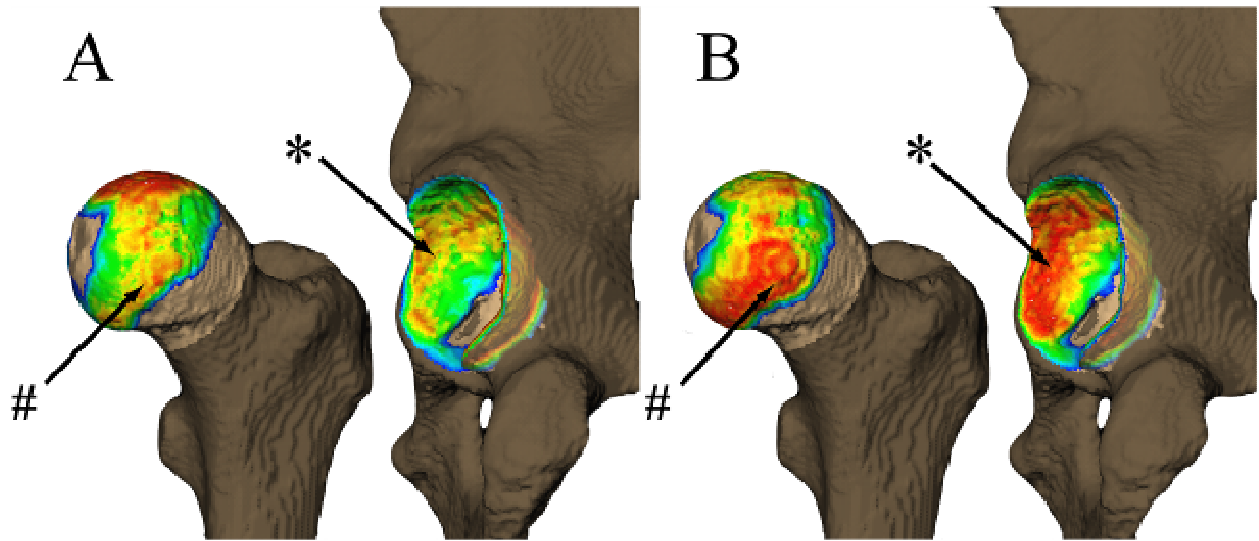
296 **Figure 3: Example of Cam Impingement**



297

298

299 **Figure 4: Hip Joint Contact Analysis in Cam Impingement**



300

301

## 302 **Figure Legend**

303

304 **Figure 1:** Normal Hip Morphology. **A:** Anteroposterior (AP) radiograph of a 23 year old female  
305 with groin pain. The center-edge angle (CEA) is measured as the angle between a vertical line  
306 that intersects the center of the femoral head and a line that is drawn from the center of the  
307 femoral head to the lateral-most aspect of the acetabulum [11]. **B:** Axial oblique slice from  
308 magnetic resonance imaging (MRI) of the same subject (orientation of slice illustrated in a  
309 coronal slice in the upper-left corner of the image). The alpha angle is measured as the angle  
310 between a line parallel to the axis of the femoral neck and a line drawn from the center of the  
311 femoral head to the point at which the distance from the center of the femoral head to the cortex  
312 of the femoral head or neck first exceeds the radius of a sphere fit to the femoral head [14]. **C:**  
313 AP radiograph of a 40 year old female with hip pain. The triangular index is calculated by first  
314 fitting a circle to the femoral head and measuring the radius of the circle ( $r$ ). A line is next drawn  
315 along the longitudinal axis of the femoral neck, and then another line is drawn perpendicularly to  
316 this line at a distance of  $r/2$  from the center of the femoral head. Finally, a triangle is drawn with  
317 a hypotenuse ( $R$ ) going from the center of the femoral head to the point at which the lateral  
318 cortex of the femur intersects the line previously drawn perpendicularly to the longitudinal axis  
319 of the femur. When a radiograph with 1.2 times magnification is used, the proximal femur is  
320 classified as abnormal when  $R \geq r + 2 \text{ mm}$  [15].

321

322 **Figure 2:** Mechanisms of Femoroacetabular Impingement. Normal morphology from an axial  
323 oblique perspective is depicted in **A**, with a lack of impingement noted when the femur is flexed  
324 anteriorly in **B**. A cam deformity (excess bone depicted in grey) in a neutral position is shown in

325 **C**, while anterosuperior impingement occurs (depicted in red) when the femur is flexed anteriorly  
326 in **D**. A pincer deformity (excess bone depicted in grey) in a neutral position is depicted in **E**,  
327 while anterosuperior impingement occurs (depicted in red) when the femur is flexed anteriorly in  
328 **F**. The combination of a cam deformity and a pincer deformity depicted in **G** may result in the  
329 contre-coup mechanism depicted in **H**, where the point of anterosuperior impingement creates a  
330 fulcrum that elevates the femoral head out of the acetabulum and causes posteroinferior  
331 impingement.

332  
333 **Figure 3:** Example of Cam Impingement. **A:** AP radiograph of a 35 year old male with groin  
334 pain. An obvious cam lesion is denoted with a “\*.” **B:** Axial MRI slice of the same subject, with  
335 an anterosuperior labral tear denoted with a “#.”

336  
337 **Figure 4:** Hip Joint Contact Analysis in Cam Impingement. Joint contact analysis for the subject  
338 in Figure 3 at 40° (**A**) and 60° (**B**) of hip flexion. Color scale from 0.1 mm (red) to 5 mm (blue).  
339 \* = anterosuperior acetabulum, # = anterior femoral head/neck junction.

## References

- 340  
341  
342 1. Chandler DR, Glousman R, Hull D, et al. Prosthetic hip range of motion and  
343 impingement. The effects of head and neck geometry. *Clin Orthop Relat Res* 1982;284.
- 344 2. Ito K, Minka MA, 2nd, Leunig M, et al. Femoroacetabular impingement and the cam-  
345 effect. A mri-based quantitative anatomical study of the femoral head-neck offset. *J Bone*  
346 *Joint Surg Br* 2001;83:171.
- 347 3. Kluess D, Martin H, Mittelmeier W, et al. Influence of femoral head size on  
348 impingement, dislocation and stress distribution in total hip replacement. *Med Eng Phys*  
349 *2007;29:465*.
- 350 4. Myers SR, Eijer HGanz R. Anterior femoroacetabular impingement after periacetabular  
351 osteotomy. *Clin Orthop Relat Res* 1999;93.
- 352 5. Fraitzl CR, Kafer W, Nelitz M, et al. Radiological evidence of femoroacetabular  
353 impingement in mild slipped capital femoral epiphysis: A mean follow-up of 14.4 years  
354 after pinning in situ. *J Bone Joint Surg Br* 2007;89:1592.
- 355 6. Ilizaliturri VM, Jr., Nossa-Barrera JM, Acosta-Rodriguez E, et al. Arthroscopic treatment  
356 of femoroacetabular impingement secondary to paediatric hip disorders. *J Bone Joint*  
357 *Surg Br* 2007;89:1025.
- 358 7. Tjoumakaris FP, Wallach DMDavidson RS. Subtrochanteric osteotomy effectively treats  
359 femoroacetabular impingement after slipped capital femoral epiphysis. *Clin Orthop Relat*  
360 *Res* 2007;464:230.
- 361 8. Ganz R, Gill TJ, Gautier E, et al. Surgical dislocation of the adult hip a technique with  
362 full access to the femoral head and acetabulum without the risk of avascular necrosis. *J*  
363 *Bone Joint Surg Br* 2001;83:1119.
- 364 9. Ganz R, Parvizi J, Beck M, et al. Femoroacetabular impingement: A cause for  
365 osteoarthritis of the hip. *Clin Orthop Relat Res* 2003;112.
- 366 10. Beck M, Kalhor M, Leunig M, et al. Hip morphology influences the pattern of damage to  
367 the acetabular cartilage: Femoroacetabular impingement as a cause of early osteoarthritis  
368 of the hip. *J Bone Joint Surg Br* 2005;87:1012.
- 369 11. Delaunay S, Dussault RG, Kaplan PA, et al. Radiographic measurements of dysplastic  
370 adult hips. *Skeletal Radiol* 1997;26:75.
- 371 12. Toomayan GA, Holman WR, Major NM, et al. Sensitivity of mr arthrography in the  
372 evaluation of acetabular labral tears. *AJR Am J Roentgenol* 2006;186:449.
- 373 13. Klaue K, Durnin CWGanz R. The acetabular rim syndrome. A clinical presentation of  
374 dysplasia of the hip. *J Bone Joint Surg Br* 1991;73:423.
- 375 14. Notzli HP, Wyss TF, Stoecklin CH, et al. The contour of the femoral head-neck junction  
376 as a predictor for the risk of anterior impingement. *J Bone Joint Surg Br* 2002;84:556.
- 377 15. Gosvig KK, Jacobsen S, Palm H, et al. A new radiological index for assessing asphericity  
378 of the femoral head in cam impingement. *J Bone Joint Surg Br* 2007;89:1309.
- 379 16. Tanzer MNoiseux N. Osseous abnormalities and early osteoarthritis: The role of hip  
380 impingement. *Clin Orthop Relat Res* 2004;170.
- 381 17. Pfirrmann CW, Mengiardi B, Dora C, et al. Cam and pincer femoroacetabular  
382 impingement: Characteristic mr arthrographic findings in 50 patients. *Radiology*  
383 *2006;240:778*.

- 384 18. Philippon MJ, Maxwell RB, Johnston TL, et al. Clinical presentation of femoroacetabular  
385 impingement. *Knee Surg Sports Traumatol Arthrosc* 2007;15:1041.
- 386 19. Beaulé PE, Le Duff MJ, Zaragoza E. Quality of life following femoral head-neck  
387 osteochondroplasty for femoroacetabular impingement. *J Bone Joint Surg Am*  
388 2007;89:773.
- 389 20. Philippon MJ, Stubbs AJ, Schenker ML, et al. Arthroscopic management of  
390 femoroacetabular impingement: Osteoplasty technique and literature review. *Am J Sports*  
391 *Med* 2007;35:1571.
- 392 21. Mardones R, Lara J, Donndorff A, et al. Surgical correction of "Cam-type"  
393 Femoroacetabular impingement: A cadaveric comparison of open versus arthroscopic  
394 debridement. *Arthroscopy* 2009;25:175.
- 395 22. Zumstein M, Hahn F, Sukthankar A, et al. How accurately can the acetabular rim be  
396 trimmed in hip arthroscopy for pincer-type femoral acetabular impingement: A cadaveric  
397 investigation. *Arthroscopy* 2009;25:164.
- 398 23. Beaulé PE, Zaragoza E, Motamedi K, et al. Three-dimensional computed tomography of  
399 the hip in the assessment of femoroacetabular impingement. *J Orthop Res* 2005;23:1286.
- 400 24. Tannast M, Kubiak-Langer M, Langlotz F, et al. Noninvasive three-dimensional  
401 assessment of femoroacetabular impingement. *J Orthop Res* 2007;25:122.
- 402 25. Kubiak-Langer M, Tannast M, Murphy SB, et al. Range of motion in anterior  
403 femoroacetabular impingement. *Clin Orthop Relat Res* 2007;458:117.
- 404 26. Wyss TF, Clark JM, Weishaupt D, et al. Correlation between internal rotation and bony  
405 anatomy in the hip. *Clin Orthop Relat Res* 2007;
- 406 27. Kennedy MJ, Lamontagne M, Beaulé PE. Femoroacetabular impingement alters hip and  
407 pelvic biomechanics during gait walking biomechanics of fai. *Gait Posture* 2009;30:41.
- 408 28. Taylor WR, Ehrig RM, Duda GN, et al. On the influence of soft tissue coverage in the  
409 determination of bone kinematics using skin markers. *J Orthop Res* 2005;23:726.
- 410 29. Mardones RM, Gonzalez C, Chen Q, et al. Surgical treatment of femoroacetabular  
411 impingement: Evaluation of the effect of the size of the resection. *J Bone Joint Surg Am*  
412 2005;87:273.
- 413 30. Harris WH. Etiology of osteoarthritis of the hip. *Clin Orthop Relat Res* 1986;20.
- 414 31. Anderson AE, Nelson DP, Weiss JA, et al., *Femoroacetabular impingement: A three-*  
415 *dimensional morphological assessment*, in *54th Annual Orthopaedic Research Society*  
416 *Meeting*. 2009: Las Vegas, Nevada.
- 417 32. Schache AG, Blanch PD, Rath DA, et al. Intra-subject repeatability of the three  
418 dimensional angular kinematics within the lumbo-pelvic-hip complex during running.  
419 *Gait Posture* 2002;15:136.
- 420 33. Leardini A, Chiari L, Della Croce U, et al. Human movement analysis using  
421 stereophotogrammetry. Part 3. Soft tissue artifact assessment and compensation. *Gait*  
422 *Posture* 2005;21:212.
- 423 34. Cappozzo A, Catani F, Leardini A, et al. Position and orientation in space of bones during  
424 movement: Experimental artifacts. *Clinical Biomechanics* 1996;11:90.
- 425 35. Taylor WR, Ehrig RM, Heller MO, et al. Tibio-femoral joint contact forces in sheep. *J*  
426 *Biomech* 2006;39:791.
- 427 36. LaFortune MA, Cavanagh PR, Sommer III HJ, et al. Three-dimensional kinematics of the  
428 human knee during walking. *J Biomech* 1992;25:347.



429 37. Steffen T, Rubin RKB, Baramki HG, et al. A new technique for measuring lumbar  
430 segmental motion in vivo: Method, accuracy, and preliminary results. *Spine* January 15  
431 1997;22:156.

432 38. Rozumalski A, Schwartz MH, Wervey R, et al. The in vivo three-dimensional motion of  
433 the human lumbar spine during gait. *Gait Posture* 2008;28:378.

434 39. Selvik G. Roentgen stereophotogrammetric analysis. *Acta Radiologica* 1990;31:113.

435 40. Tashman S, Kolowich P, Collon D, et al. Dynamic function of the acl-reconstructed knee  
436 during running. *Clin Orthop Relat Res* 2007;454:66.

437 41. Anderst WJ, Vaidya RTashman S. A technique to measure three-dimensional in vivo  
438 rotation of fused and adjacent lumbar vertebrae. *Spine J* 2008;8:991.

439 42. Bey MJ, Zael R, Brock SK, et al. Validation of a new model-based tracking technique  
440 for measuring three-dimensional, in vivo glenohumeral joint kinematics. *J Biomech Eng*  
441 2006;128:604.

442 43. Anderst W, Zael R, Bishop J, et al. Validation of three-dimensional model-based tibio-  
443 femoral tracking during running. *Med Eng Phys* 2008;

444 44. Bey MJ, Kline SK, Tashman S, et al. Accuracy of biplane x-ray imaging combined with  
445 model-based tracking for measuring in-vivo patellofemoral joint motion. *J Orthop Surg*  
446 2008;3:38.

447 45. Martin DE, Greco NJ, Klatt BA, et al. Model-based tracking of the hip: Implications for  
448 novel analyses of hip pathology. *Journal of Arthroplasty* 2010;In press:  
449  
450